FRACTURE BEHAVIOR OF FeAlSi INTERMETALLICS

Jaroslav Čech[a,*], Petr Haušild[a], Miroslav Karlík[a], Kateřina Nová[b],
Filip Průša[b], Pavel Novák[b], Jaromír Kopeček[c]

[a] *Czech Technical University in Prague, Faculty of Nuclear Sciences and Physical Engineering, Department of Materials, Trojanova 13, 120 00 Prague, Czech Republic*

[b] *University of Chemistry and Technology Prague, Faculty of Chemical Technology, Department of Metals and Corrosion Engineering, Technická 5, 166 28 Prague, Czech Republic*

[c] *Institute of Physics, ASCR, v.v.i., Department of Functional Materials, Na Slovance 2, 182 21 Prague, Czech Republic*

* corresponding author: jaroslav.cech@fjfi.cvut.cz

ABSTRACT. The study is devoted to the intermetallic alloy FeAl20Si20 (wt.%) with the potential applications in high temperature aggressive environments. The samples of the same chemical composition were prepared by spark plasma sintering from the different mechanically alloyed powders (pure elements and pre-alloyed powders). Differences in mechanical properties were characterized. Whereas no significant differences were found in hardness and Young´s modulus, fracture resistance was higher for the samples from pre-alloyed powders in which Palmqvist and lateral cracks were observed (contrary to the sample made of pure elements where only Palmqvist cracks were identified).

KEYWORDS: FeAlSi, fracture toughness, nanoindentation, SPS.

1. INTRODUCTION

Iron aluminides are one of the most studied intermetallics [1, 2], but not much attention was paid on their ternary alloys with silicon because of their brittleness. Despite this drawback, they exhibit promising mechanical properties and excellent high-temperature oxidation resistance [3]. Potential replacement of stainless steels or nickel-based superalloys would be possible only if the production process will be more effective and the brittleness significantly improved.

The standard metallurgical processes (e.g. casting and rolling) for the production of FeAlSi alloys are not convenient. For this reason, powder metallurgy, especially mechanical alloying (MA) with consequent spark plasma sintering (SPS) seems to be potentially applicable processing way. Severe deformation, repeated cold welding, fracturing and rewelding of the initial powders during mechanical alloying result in the production of homogeneous powders with fine microstructure [4, 5]. SPS used for the consolidation of the powders is very fast sintering method which reduces grain coarsening and phase changes during the sample compaction.

Resulting very fine microstructure can improve fracture toughness of these alloys which is usually very low (comparable with glasses or ceramics). As this material is brittle, the cracks are usually observed around the residual imprints after indentation measurements. Measuring their geometry can be used for the evaluation of the fracture toughness. Various methods and formulas were proposed for the determination of fracture toughness from indentation measurements (e.g. [6]). They are usually based on the size

of Palmqvist (radial) or median cracks. [7–9]. Lateral cracks [10] or energetic methods [11, 12] are used less often and proper formula has to be employed to meet the assumptions of the specific cracking system. In this study, FeAl20Si20 intermetallic alloy prepared by mechanical alloying and spark plasma sintering from various initial powders was studied. The focus was on the fracture properties investigated by indentation and scratch tests.

2. EXPERIMENTAL METHODS

2.1. MATERIAL

Three powder mixtures were prepared by mechanical alloying (MA). The final chemical composition was 60 wt.% of Fe, 20 wt.% of Al and 20 wt.% of Si (FeAl20Si20 wt.%). Differences were in the initial powders used for milling. The mixture denoted Fe_Al_Si was prepared from pure elements Fe, Al and Si. The mixture FeAl_Si was mixed from FeAl25 (wt.%) pre-alloyed powder and pure Si. The third mechanically alloyed powder (denoted FeSi_Al) was milled from FeSi25 (wt.%) pre-alloyed powder and pure Al. The powders were milled in planetary ball mill PM 100 CM (Retsch, Haan, Germany) for 8 h. Powder to ball mass ratio was 1:60, rotational speed 400 rpm and no lubricant was used to fulfill the conditions of so-called ultra-high energy mechanical alloying [13] which can reduce the time necessary for the homogenization of the powders. The shortest time for the homogenization of the powders (evaluated from X-ray diffraction, microstructural observations and nanoindentation measurements) was needed for the mixture Fe_Al_Si (4 h), for the mixture FeSi_Al

it was about 6 h, and the longest time (8 h) was necessary for the mixture FeAl_Si. The details about the powder preparation and homogenization can be found in [14].

The powders were consequently sintered by spark plasma sintering (SPS) in HP D10 device (FCT Systeme GmbH, Rauenstein, Germany). The heating rate (300 °C/min up to 900 °C and then 100 °C/min to 1000 °C), hold on the maximum temperature 1000 °C for 10 minutes, and the cooling rate (50 °C/min) were carefully adjusted to avoid temperature overshoot or cracking caused by thermal shocks.

2.2. Characterization Techniques

The compacted samples for microstructure characterization, microindentation and scratch measurements were prepared by standard metallographic procedures with the final polishing by colloidal silica suspension (0.04 μm). The microstructure was observed in light optical (Neophot 32) and scanning electron microscope (SEM) JEOL JSM 5510LV in the signal of backscattered electrons (BSE). Microindentation and scratch tests were carried out on MCT tester (Anton Paar, Graz, Austria). Maximum load for indentation with Vickers indenter was 5 N, loading and unloading rate 10 N/min and hold period at the maximum load 10 s. At least nine indentations per sample were performed. The acquired data (force F - penetration depth h dependency) were evaluated to obtain hardness H and Young´s modulus E according to the ISO 14577 standard [15] by the Oliver-Pharr method [16]. The Poisson ratio of FeAlSi samples was assumed 0.3. Fracture toughness was evaluated from the system of Palmqvist cracks observed and measured after the indentation tests. No cracks under the residual imprint were observed and only the Palmqvist cracks were confirmed by optical, electron and confocal microsopy. The equation introduced by Niihara [7] was used to calculate the values of K_{IC}:

$$ K_{IC} = 0.035 \left(\frac{l}{a} \right) H a^{1/2} \frac{1}{\phi} \left(\frac{E\phi}{H} \right)^{2/5}, \qquad (1) $$

where l is the crack length, a is the half-diagonal of the indent (see Figure 1) and ϕ stands for the constraint factor (assumed to equal to 3). This formula is valid for the Palmqvist cracks and the crack lengths $0.25 \leq l/a \leq 2.5$.

Three scratches were performed for every sample to obtain statistically relevant data about scratch resistance. The scratches of the length 1 mm with the progressively increasing load from 0.03 N up to 30 N were carried out by Rockwell sphero-conical diamond indenter with radius 100 μm. No lubricant was used during scratch tests. The data of the depth, normal and friction load were recorded by the instrument during every test. Pre-scan and Post-scan procedures [18] (i.e. scanning of the surface topography at the location of the scratch by load 0.03 N before and after the
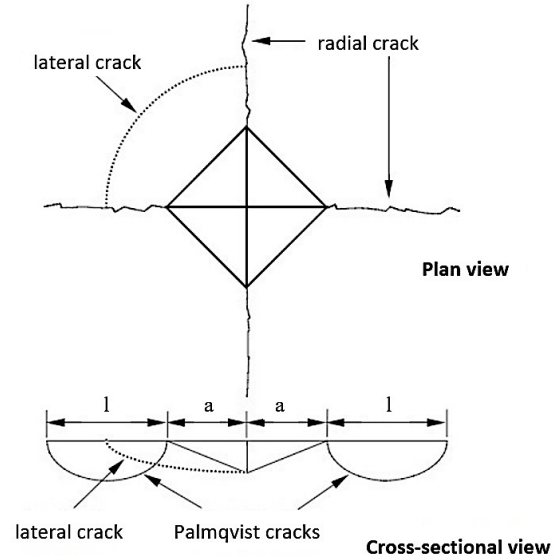
Figure 1. Palmqvist and lateral crack systems (adapted from [17]).

test) enabled measuring of the correct values of penetration and residual depth not affected by the surface profile. The panorama images of the scratch, which correlate the measured signals with optical image and enable the subsequent evaluation of the data, were taken. Critical load L_c denoting the cracking load of the samples was consequently determined from the optical analysis.

3. Results and Discussion

3.1. Indentation

Spark plasma sintering was chosen as a compaction method as it is fast and it prevents the coarsening of the fine microstructure obtained by mechanical alloying. The microstructure observations revealed very fine structure with the equiaxed grains of mean size approximately 1 μm for all the samples. Fine-grained microstructure resulted in very good mechanical properties (Table 1).

No significant differences in hardness and Young´s modulus were found between the sintered compacts. Young´s modulus was approximately 220 GPa for the samples from pre-alloyed powders, slightly higher (234 GPa) for the sample from pure elements. The values of the Young´s modulus are close to Young´s modulus of the steel, which is suitable for the potential replacement of the steel products by this intermetallic alloy. Moreover, the measured hardness of the FeAlSi samples was about 13 GPa (only slightly lower for the sample FeSi_Al) which is higher than for common steels and it can be beneficial in some applications.

On the other hand, intermetallic alloys are usually very brittle and they have low fracture toughness which is very limiting for practical use of these alloys. This was confirmed for the studied alloy for

	H [GPa]	E [GPa]	l/a [−]	K_{IC} [MPa.m$^{1/2}$]	L_c [N]
Fe__Al__Si	13.48 ± 0.44	233.55 ± 6.47	1.28 ± 0.15	2.57 ± 0.18	11.8 ± 0.5
FeAl__Si	13.46 ± 0.25	220.45 ± 1.71	0.62 ± 0.09	3.61 ± 0.32	16.1 ± 0.8
FeSi__Al	12.61 ± 0.15	220.66 ± 2.96	0.74 ± 0.18	3.21 ± 0.40	22.7 ± 0.8

TABLE 1. Mechanical properties of FeAl20Si20 samples.
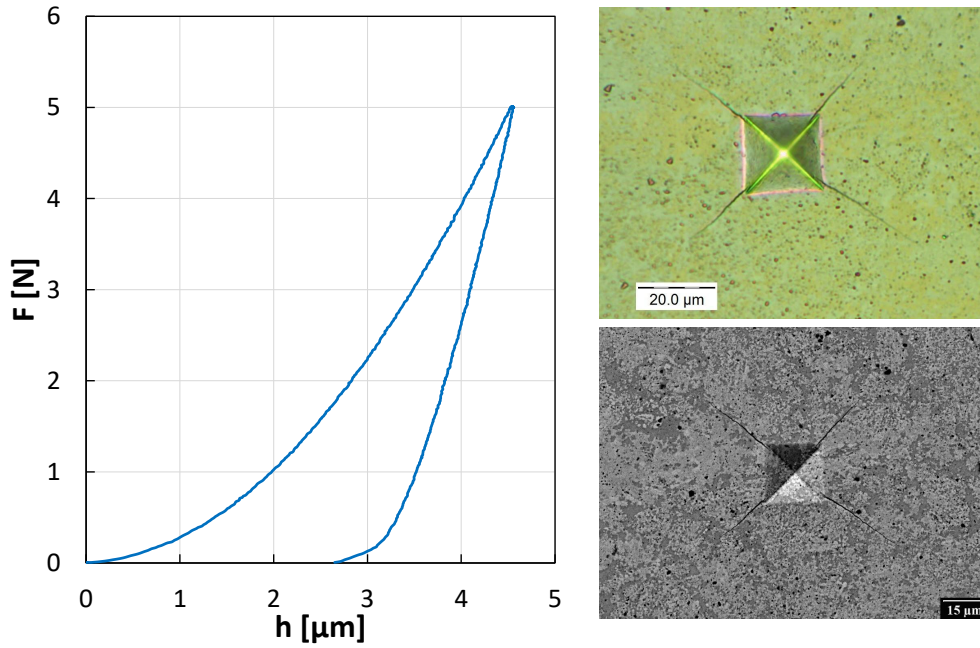
FIGURE 2. Indentation curve and the residual indent with Palmqvist cracks in Fe__Al__Si sample. No lateral cracks were observed on micrographs from light optical microscope or SEM.
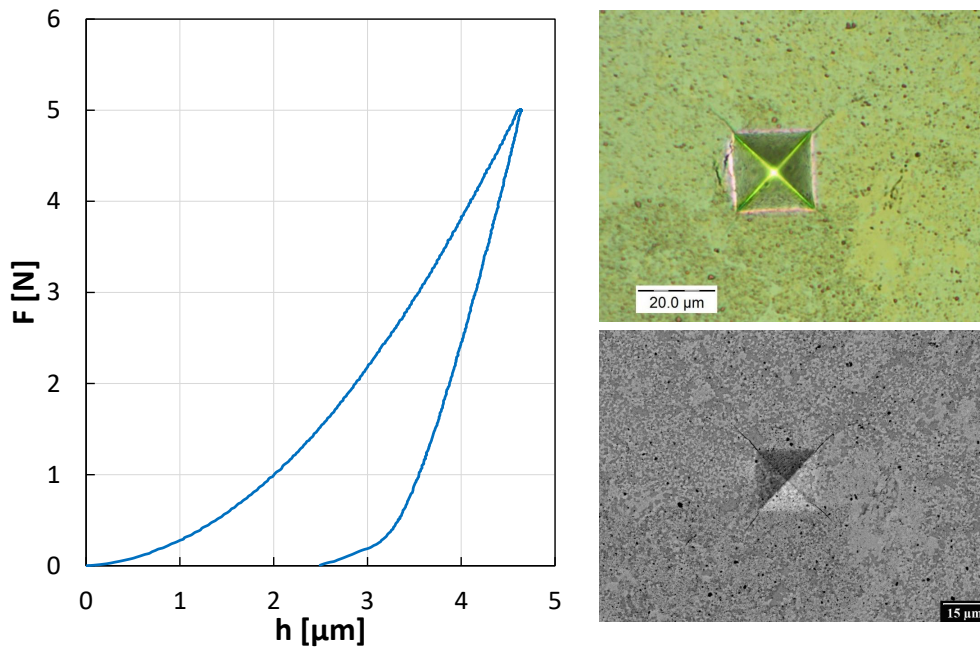
FIGURE 3. Indentation curve and the residual indent with Palmqvist and lateral cracks in FeAl__Si sample. Lateral cracks are visible on light optical micrographs.
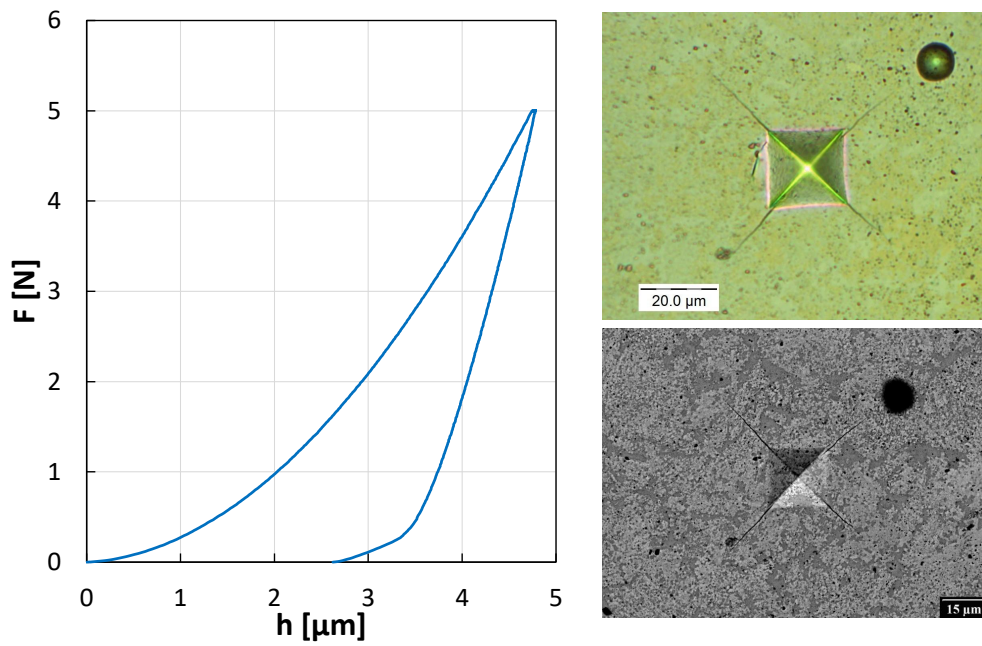
FIGURE 4. Indentation curve and the residual indent with Palmqvist and lateral cracks in FeSi_Al sample. Lateral cracks are visible on light optical micrographs.
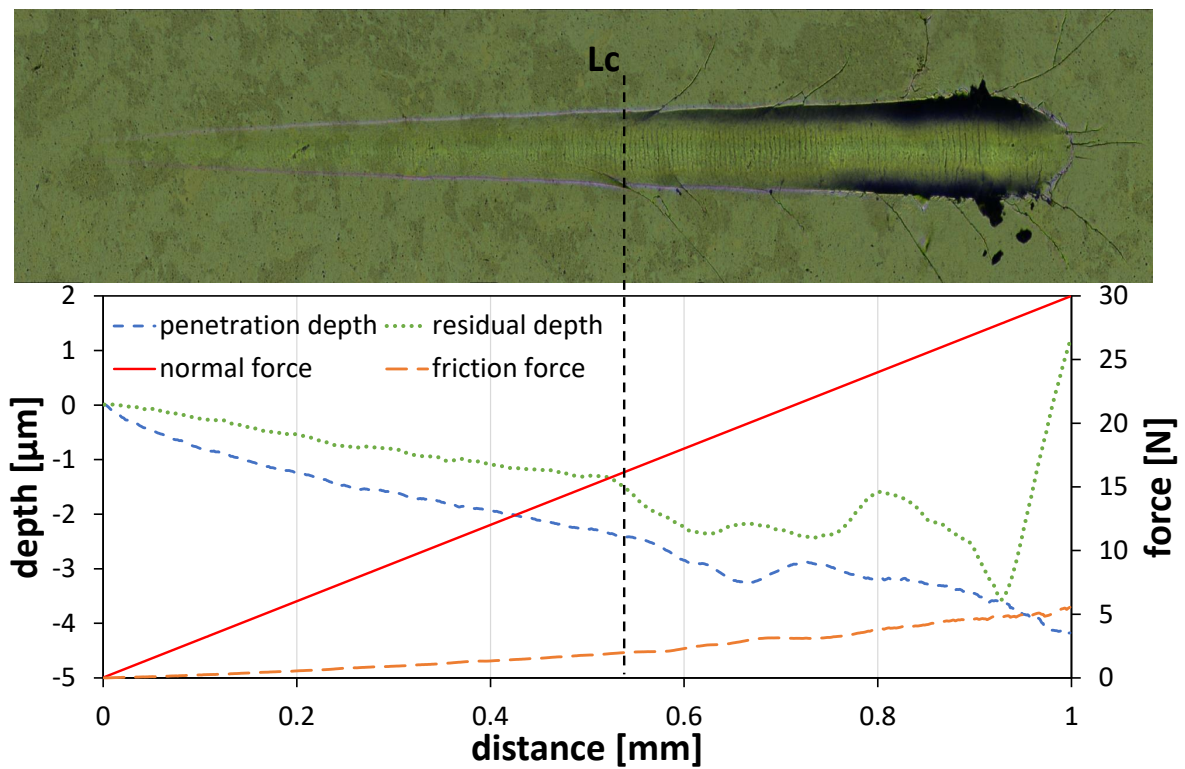
FIGURE 5. Scratch panorama and measured signals on FeAl_Si sample.
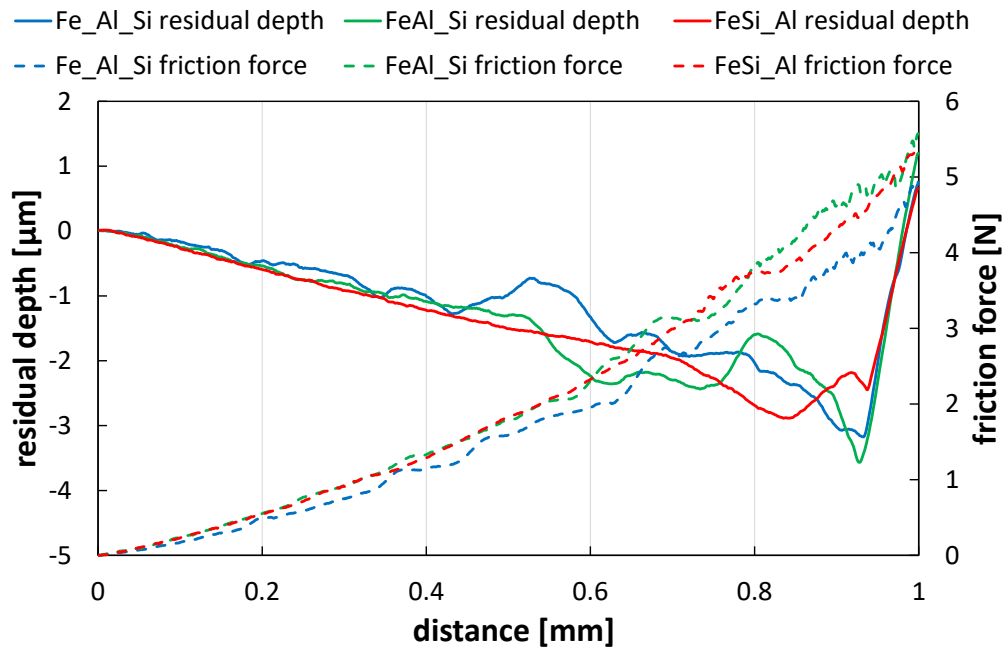
FIGURE 6. Comparison of residual depth and friction force.
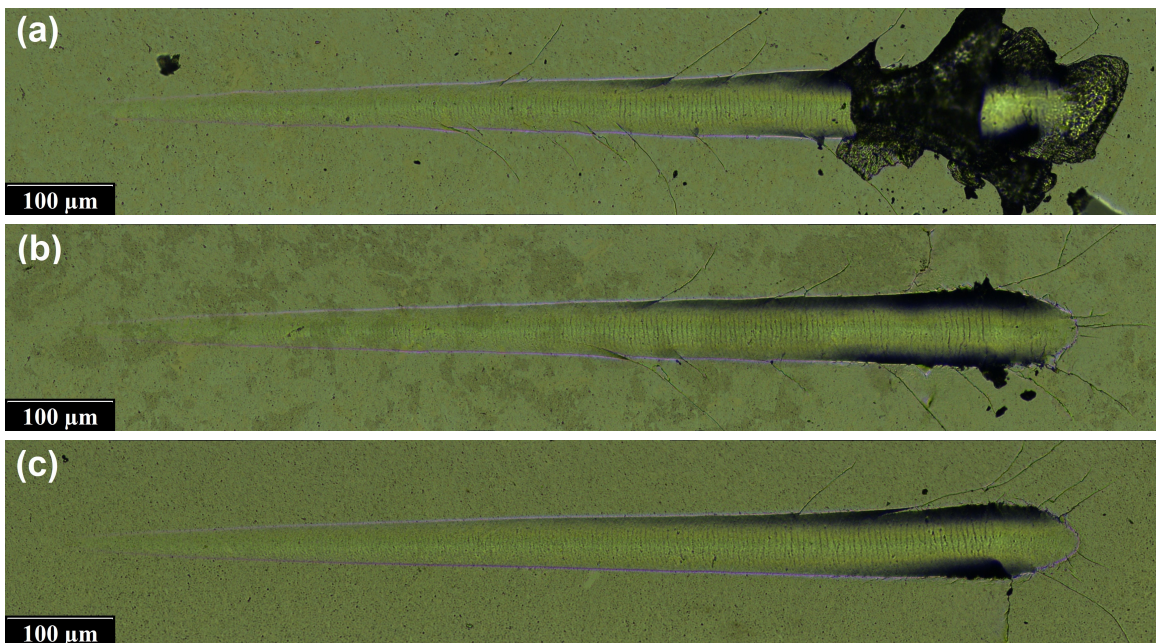
FIGURE 7. Scratches on (a) Fe_Al_Si, (b) FeAl_Si and (c) FeSi_Al samples.

which the measured values of fracture toughness were around $3\,\mathrm{MPa.m}^{1/2}$. Even if this value is about ten times higher than fracture toughness of casted FeAlSi alloys [19], it is still very low value.

Some differences in the values of fracture toughness and developed crack systems were found between the samples from pure and pre-alloyed powders (Table 1, Figures 2, 3 and 4). Even if the indentation force-penetration depth curves are very similar and no pop-ins associated with the cracking can be observed, the various cracks were identified after the optical analysis. For Fe_Al_Si sample, only Palmqvist cracks initiated in all four corners of the residual imprint were observed and the calculated fracture toughness reached the lowest value ($2.6\,\mathrm{MPa.m}^{1/2}$). The samples from pre-alloyed powders had higher fracture toughness ($3.2\,\mathrm{MPa.m}^{1/2}$ for FeSi_Al sample and $3.6\,\mathrm{MPa.m}^{1/2}$ for FeAl_Si sample) and for some indents, the Palmqvist cracks propagated only form 3 corners of the imprint. In these cases, lateral cracks were often observed. Differences in the fracture behavior can be probably attributed to the amount of the stored plastic deformation during mechanical alloying of the powders [14]. The homogenization of the Fe_Al_Si powder was the fastest and after its end, no microstructural changes were observed and only plastic deformation was accumulated in the powder. The homogenization of the samples FeAl_Si and FeSi_Al was more progressive [14], it took more time and less plastic deformation causing the brittleness of the samples was stored in the powders.

3.2. SCRATCH RESISTANCE

Typical example of the scratch correlated with measured signals is shown in Figure 5. No significant differences between samples were found in the depth or friction force signals (Figure 6). The coefficient of friction progressively increased from approximately 0.05 at the beginning of the test to the value of nearly 0.2 at maximum load for all tested samples. The small cracks inside the scratch path were observed from the lowest applied loads for all samples. Critical load L_c was optically determined as the normal load measured at the position where the large long crack gets outside the scratch path (Figure 5). At this position, the fast increase in residual depth was also found. The values of critical loads are summarized in Table 1 and the typical panorama images are presented in Figure 7. Same as for the indentation fracture toughness, lowest critical load was found for Fe_Al_Si sample from pure elements. At higher loads, total destruction of the sample (Figure 7a) was observed for some scratches. This failure has the character of chipping and crumbling of the sample. Samples from pre-alloyed powders showed higher scratch resistance (higher critical load) and no evidence of chipping.

4. CONCLUSIONS

The FeAl20Si20 samples were prepared by spark plasma sintering form various initial powders (pure elements Fe, Al, Si and pre-alloyed FeAl25 and FeSi25). Mechanical properties including hardness, Young´s modulus, fracture toughness and scratch resistance were measured. No significant differences between the samples were found in hardness and Young´s modulus. The fracture toughness and scratch resistance were higher for the samples made of pre-alloyed powders than for the sample milled from pure elements proving the importance of processing route on mechanical properties.

REFERENCES

[1] S. Deevi, V. Sikka. Nickel and iron aluminides: An overview on properties, processing, and applications. *Intermetallics* **4**:357–375, 1996. DOI:10.1016/0966-9795(95)00056-9.

[2] X. Zhu, Z. Yao, X. Gu, et al. Microstructure and corrosion resistance of Fe-Al intermetallic coating on 45 steel synthesized by double glow plasma surface alloying technology. *Trans of Nonferrous Met Soc China* **19**:143–148, 2009. DOI:10.1016/S1003-6326(08)60242-3.

[3] P. Novák, M. Zelinková, J. Šerák, et al. Oxidation resistance of SHS Fe-Al-Si alloys at 800 °C in air. *Intermetallics* **19**:1306–1312, 2011. DOI:10.1016/j.intermet.2011.04.011.

[4] C. Suryanarayana. Mechanical alloying and milling. *Prog Mater Sci* **46**:1–184, 2001. DOI:10.1016/S0079-6425(99)00010-9.

[5] L. Bhadeshia. Mechanically alloyed metals. *Mater Sci Technol* **16**:1404–1411, 2000. DOI:10.1179/026708300101507361.

[6] S. Zhang, X. Zhang. Toughness evaluation of hard coatings and thin films. *Thin Solid Films* **520**:2375–2389, 2012. DOI:10.1016/j.tsf.2011.09.036.

[7] K. Niihara. A fracture mechanics analysis of indentation-induced palmvist crack in ceramics. *J Mater Sci Lett* **2**:221–223, 1983. DOI:10.1007/BF00725625.

[8] M. Laugier. New formula for indentation toughness in ceramics. *J Mater Sci Lett* **6**:355–356, 1987. DOI:10.1007/BF01729352.

[9] B. Lawn, A. Evans, D. Marshall. Elastic/plastic indentation damage in ceramics: The median/radial crack system. *J Am Ceram Soc* **63**:574–581, 1980. DOI:10.1111/j.1151-2916.1980.tb10768.x.

[10] D. Marshall, B. Lawn, A. Evans. Elastic/plastic indentation damage in ceramics: The lateral crack system. *J Am Ceram Soc* **65**:561–566, 1982. DOI:10.1111/j.1151-2916.1982.tb10782.x.

[11] J. Malzbender, G. de With. Energy dissipation, fracture toughness and the indentation load-displacement curve of coated materials. *Surf Coat Technol* **135**:60–68, 2000. DOI:10.1016/S0257-8972(00)00906-3.

[12] J. Chen, S. Bull. Assessment of the toughness of thin coatings using nanoindentation under displacement control. *Thin Solid Films* **494**:1–7, 2006. DOI:10.1016/j.tsf.2005.08.176.

[13] P. Novák, F. Průša, K. Nová, et al. Application of mechanical alloying in synthesis of intermetallics. *Acta Phys Pol A* **134**:720–723, 2018. DOI:10.12693/APhysPolA.134.720.

[14] J. Čech, P. Haušild, M. Karlík, et al. Effect of initial powders on properties of FeAlSi intermetallics. *Materials* **12**:16, 2019. DOI:10.3390/ma12182846.

[15] ISO 14557, Metallic materials - Instrumented indentation test for hardness and material parameters, 2002.

[16] W. C. Oliver, G. M. Pharr. An improved technique for determining hardness and elastic modulus using load and displacement sensing indentation experiments. *J Mater Res* **7**:1564–1583, 1992. DOI:10.1557/JMR.1992.1564.

[17] K. Jin, M. Minggat, R. Singh. Sintered properties of stainless steel-doped Y-TZP ceramics. *MATEC Web of Conferences* **152**:13, 2018. DOI:10.1051/matecconf/201815202012.

[18] Anton Paar. *Scratch Software Manual V8*, 2019.

[19] K. Nová, P. Novák, T. Vanka, F. Průša. The effect of production process on properties of FeAl20Si20. *Manuf Technol* **18**:295–298, 2018. DOI:10.21062/ujep/94.2018/a/1213-2489/MT/18/2/295.